Mapping human preictal and ictal haemodynamic networks using simultaneous intracranial EEG-fMRI

Chaudhary, Umair J; Centeno, Maria; Thornton, Rachel C; Rodionov, Roman; Vulliemoz, Serge; McEvoy, Andrew W; Diehl, Beate; Walker, Matthew C; Duncan, John S; Carmichael, David W; Lemieux, Louis

How to cite

CHAUDHARY, Umair J et al. Mapping human preictal and ictal haemodynamic networks using simultaneous intracranial EEG-fMRI. In: NeuroImage: Clinical, 2016, vol. 11, p. 486–493. doi: 10.1016/j.nicl.2016.03.010

This publication URL: https://archive-ouverte.unige.ch/unige:126158
Publication DOI: 10.1016/j.nicl.2016.03.010

NeuroImage: Clinical 11 (2016) 486–493

Contents lists available at ScienceDirect

NeuroImage: Clinical

journal homepage: www.elsevier.com/locate/ynicl

Mapping human preictal and ictal haemodynamic networks using simultaneous intracranial EEG-fMRI

Umair J. Chaudhary[a,b,1], Maria Centeno[a,b,c,*,1], Rachel C. Thornton[a,b], Roman Rodionov[a,b], Serge Vulliemoz[d], Andrew W. McEvoy[e], Beate Diehl[a,b,f], Matthew C. Walker[a,b], John S. Duncan[a,b], David W. Carmichael[c], Louis Lemieux[a,b]

[a] Department of Clinical and Experimental Epilepsy, UCL Institute of Neurology, Queen Square, London, UK
[b] MRI Unit, Epilepsy Society, Chalfont St. Peter, UK
[c] Imaging and Biophysics Unit, UCL Institute of Child Health, London, UK
[d] EEG and Epilepsy Unit, Neurology, University Hospital and Functional Brain Mapping Lab, Faculty of Medicine, Geneva, Switzerland
[e] Victor Horsley Department of Surgery, National Hospital for Neurology and Neurosurgery, Queen Square, London, UK
[f] Clinical Neurophysiology, National Hospital for Neurology and Neurosurgery, Queen Square, London, UK

ARTICLE INFO

Article history:
Received 1 October 2015
Received in revised form 4 March 2016
Accepted 11 March 2016
Available online 23 March 2016

ABSTRACT

Accurately characterising the brain networks involved in seizure activity may have important implications for our understanding of epilepsy. Intracranial EEG-fMRI can be used to capture focal epileptic events in humans with exquisite electrophysiological sensitivity and allows for identification of brain structures involved in this phenomenon over the entire brain. We investigated ictal BOLD networks using the simultaneous intracranial EEG-fMRI (icEEG-fMRI) in a 30 year-old male undergoing invasive presurgical evaluation with bilateral depth electrode implantations in amygdalae and hippocampi for refractory temporal lobe epilepsy. One spontaneous focal electrographic seizure was recorded. The aims of the data analysis were firstly to map BOLD changes related to the ictal activity identified on icEEG and secondly to compare different fMRI modelling approaches.

Visual inspection of the icEEG showed an onset dominated by beta activity involving the right amygdala and hippocampus lasting 6.4 s (*ictal onset phase*), followed by gamma activity bilaterally lasting 14.8 s (*late ictal phase*). The fMRI data was analysed using SPM8 using two modelling approaches: firstly, purely based on the visually identified phases of the seizure and secondly, based on EEG spectral dynamics quantification. For the visual approach the two ictal phases were modelled as 'ON' blocks convolved with the haemodynamic response function; in addition the BOLD changes during the 30 s preceding the onset were modelled using a flexible basis set. For the quantitative fMRI modelling approach two models were evaluated: one consisting of the variations in beta and gamma bands power, thereby adding a quantitative element to the visually-derived models, and another based on principal components analysis of the entire spectrogram in attempt to reduce the bias associated with the visual appreciation of the icEEG.

BOLD changes related to the visually defined ictal onset phase were revealed in the medial and lateral right temporal lobe. For the late ictal phase, the BOLD changes were remote from the SOZ and in deep brain areas (precuneus, posterior cingulate and others). The two quantitative models revealed BOLD changes involving the right hippocampus, amygdala and fusiform gyrus and in remote deep brain structures and the default mode network-related areas.

In conclusion, icEEG-fMRI allowed us to reveal BOLD changes within and beyond the SOZ linked to very localised ictal fluctuations in beta and gamma activity measured in the amygdala and hippocampus. Furthermore, the BOLD changes within the SOZ structures were better captured by the quantitative models, highlighting the interest in considering seizure-related EEG fluctuations across the entire spectrum.

1. Introduction

Seizures are transient episodes of abnormal excessive or synchronous neuronal activity in the brain (Fisher et al., 2005). Seizure generation and propagation involves evolving abnormal synchronization between regions at the seizure onset (Schindler et al., 2007) which

* Corresponding author at: MRI Unit, Epilepsy Society, Chalfont St. Peter SL9 0RJ, UK.
E-mail address: m.centeno@ucl.ac.uk (M. Centeno).
[1] Umair Chaudhary and Maria Centeno have made equal contributions to the work.

http://dx.doi.org/10.1016/j.nicl.2016.03.010
2213-1582/

may vary from de-synchronization (deCurtis and Gnatkovsky, 2009; Gnatkovsky et al., 2008; Mormann et al., 2003; Niedermeyer, 2005; Truccolo et al., 2011; Wendling et al., 2003) to synchronization/hyper-synchronization (Babb et al., 1987).

The regions involved in the generation and propagation of ictal activity can be investigated with intracranial-EEG (icEEG) however it suffers from limited spatial sampling. Characterising the regions involved in this process would be a great advance in understanding epilepsy.

Simultaneous scalp electroencephalography and functional MRI (EEG-fMRI) has revealed often complex patterns of the blood-oxygen-level-dependent (BOLD) changes, involving both SOZ and remotely, associated with interictal (Thornton et al., 2011; Tyvaert et al., 2008) and ictal (Tyvaert et al., 2008; Chaudhary et al., 2012; Thornton et al., 2010) activity in patients with focal epilepsy. However electrical ictal changes may show significantly delay (Tao et al., 2007) or be undetected (Smith, 2005) on scalp EEG.

A recent development has been the implementation of simultaneous recording of icEEG and fMRI (icEEG-fMRI) (Carmichael et al., 2012; Vulliemoz et al., 2011; Cunningham et al., 2012) demonstrating significant BOLD changes for very focal interictal epileptiform discharges (IED).

Here we report on a patient who had a focal electrographic seizure limited to a few electrode contacts during icEEG-fMRI. Electrographic seizures are defined as those visible on EEG but that have no clinical correlates. In order to obtain a more complete characterisation of seizure dynamics, fMRI mapping was performed based on two modelling approaches: first, by modelling the BOLD changes corresponding to the seizure phases identified by visual inspection, and second, based on the quantification of EEG dynamics during the event.

The aims of the proposed analysis were firstly, to investigate the whole-brain BOLD changes related to the observed very focal ictal activity identified on icEEG and secondly to compare the different modelling approaches (visual vs quantitative) of EEG in their ability to capture BOLD changes in the seizure onset zone.

2. Methods

2.1. Patient selection

We report on a 30 year-old, right-handed male undergoing intracranial-EEG recordings as part of presurgical evaluation for refractory temporal lobe epilepsy at the National Hospital for Neurology and Neurosurgery (UCLH NHS Foundation Trust, Queen Square, London, UK). He was part of series of 18 patients who had no contraindications (Carmichael et al., 2010, 2012) and gave informed written consent to undergo icEEG-fMRI. He was selected for this analysis because uniquely in this series, he had an electrographic seizure recorded during icEEG-fMRI. The patient underwent standard presurgical evaluation including detailed history taking, neurological examination, long-term video-EEG monitoring, MRI and neuropsychological and neuropsychiatric assessment. He had undergone scalp EEG-fMRI recording prior to the invasive investigations. The clinical and icEEG implantation details are described in Table 1. The patient had interictal discharges and seizures from bilateral temporal lobes independently. The patient's clinical seizures, and some electrographic seizures, arose from the left temporal lobe; other electrographic seizures arose independently from the right temporal lobe. No clinical seizures were recorded from the right temporal lobe. The seizure presented in this study was an electrographic seizure arising from the right temporal lobe. Electrographic seizures are defined as those visible on EEG but that have no clinical correlates. The patient was free of clinical seizures 4 years after left temporal lobe resection, which was performed following the investigation reported here. Antiepileptic medications were reduced by 50% only at 2 years post-surgery. Although the patient was free of clinical seizures it is likely electrical seizures may still occurring from the right medial temporal lobe, however these have not been further investigated with EEG after surgery since the clinical symptoms have been under control.

Table 1
Clinical details.

Investigation	Findings	
Detailed history taking	Early development: premature birth by 4 weeks and febrile convulsion at age 18 months Seizure onset: Age 7 years Seizure type: Focal dyscognitive seizures Epigastric aura > automotor seizure > hypermotor seizure (with loss of awareness), no lateralizing signs	
Neurological examination	No abnormality detected	
Long-term video EEG monitoring	Interictal spikes Bi temporal sharp waves	Seizure EEG ictal onset: regional left temporal (rhythmic slowing: left anterior temporal region) Initial clinical semiology was consistent with temporal lobe seizures, however later it was more suggestive of extra-temporal lobe seizures.
Structural MRI scan	Left hippocampal sclerosis Hippocampal volumes: small for both hippocampi	
Neuropsychology	Relatively weak verbal memory with some frontal executive dysfunction	
Neuropsychiatry	No abnormality detected	
Scalp EEG-fMRI	Using spike based conventional general linear model analysis {Chaudhary, 2012 925/id} BOLD changes were seen in left posterior middle temporal gyrus associated with left temporal sharp waves.	
Intracranial EEG: 1. Left amygdala (LA) 2. Left anterior hippocampus (LAH) 3. Left posterior hippocampus (LPH) 4. Right amygdala (RA) 5. Right hippocampus (RH)Each depth electrode contains 6 contacts; 1 being most medial and 6 being most lateral	Interictal spikes • Right amygdala • Right hippocampus • Left anterior hippocampus • Left posterior hippocampus Irritative zones • Right amygdala • Right hippocampus • Left anterior hippocampus • Left posterior hippocampus	Clinical seizures • Onset from left anterior hippocampus with focal fast activity. Subclinical electrographic seizures • Independent onset from 1. Left anterior hippocampus 2. Right amygdalaSeizure onset zone • Left anterior hippocampus (clinical seizures) • Left anterior hippocampus (electrographic seizures) • Right amygdala (electrographic seizures) Epileptogenic zone • Left anterior hippocampus
Surgery	Procedure Left anterior temporal lobe resection	Outcome Seizure free at 50 months postsurgically

2.2. icEEG-fMRI acquisition

After clinical icEEG recordings were completed, the implanted electrodes were connected to MR scanner-compatible amplifier system (Carmichael et al., 2012; Vulliemoz et al., 2011; Carmichael et al., 2010). IcEEG was recorded and displayed (BrainVision Recorder and RecView, Brain Products, Germany) during fMRI. In accordance with our icEEG-fMRI protocol two ten-minute resting state echo planar images (EPI) time series and T1-weighted structural scans were acquired using a 1.5 Tesla scanner (Siemens, Erlangen, Germany) with a quadrature transmit/receive head-coil and low specific absorption rate sequences (≤0.1 W/kg head average) (Carmichael et al., 2008, 2010, 2012).

2.3. Visual icEEG interpretation and fMRI pre-processing

The scanner-related artefact corrected intracranial EEG (Allen et al., 2000) was reviewed by experts (BD, MW, UC) to identify interictal and ictal epileptic activity using Brain Vision Analyzer2 (Brain Products, Germany) and compared with long-term icEEG monitoring. IEDs were identified and classified according to their spatiotemporal distribution. Two left temporal and one right temporal IED types were identified in agreement with the findings in the clinical icEEG study. IED were included in the fMRI models to account for the effect of this activity.

The electrographic seizure was identified and partitioned into two distinct ictal phases: *ictal onset* and *late ictal* (Chaudhary et al., 2012), according to their spatial and temporal characteristics involving different electrode contacts on icEEG. The *ictal onset phase* was characterised by relatively prominent beta activity (16 Hz) apparent at contacts RA 1–4 and RH 1–2 (duration = 6.4 s). The *late ictal phase* was characterised by prominent fast activity (gamma band: 49 Hz) visible at contacts RA 1–2, RH 1–2 and left posterior hippocampus (LPH) 4–5 (duration = 14.8 s).

The SOZ and IZ were defined based on the clinical icEEG assessment (see Table 1).

The fMRI data was analysed using Statistical Parametric Mapping (SPM) software version 8 (www.fil.ion.ucl.ac.uk) after discarding the first two volumes to avoid T1-saturation effects. The imaging time series data were corrected for slice acquisition time, realigned to the mean and spatially smoothed using an isotropic Gaussian-kernel of 8 mm FWHM (Friston et al., 1995).

2.4. fMRI modelling of the visually identified ictal and preictal phases

In addition to the two ictal phases, and following our previous work (Chaudhary et al., 2012), a preictal phase was defined covering the period starting 30 s prior to, and up to the first ictal electrographic change (i.e., start of the *ictal onset phase*) on icEEG. Two general linear models (GLM) were used to investigate the BOLD changes associated with the visually defined ictal and preictal phases:

- *Model 1 Ictal changes*: Each ictal phase was represented mathematically as variable-duration block and each IED type (either as stick functions and blocks for runs) as a separate regressor. To explain as much of the BOLD signal variance as possible, this model also included regressors of no interest representing motion (inter-scan realignment parameters and their Volterra expansion (Friston et al., 1996)) and cardiac pulse (Liston et al., 2006). Ictal phases and spikes were convolved with the canonical haemodynamic response function and its derivatives (Friston et al., 1994). We used a segmented T1 structural mask co-registered to EPI, to limit our study to ictal and IED-related BOLD changes located in the grey matter. The fMRI data was high-pass filtered (cut-off: 128 s).
- *Model 2 Preictal changes*: A Fourier-basis-set was used to flexibly model possible BOLD changes during the preictal phase defined as 30 s prior to the *ictal onset phase*. The regressors of *model 1* were included in the design matrix of *model 2* as confounds (Chaudhary et al., 2012).

2.5. fMRI modelling: seizure spectral dynamics

fMRI mapping of quantitative EEG characteristics was performed by constructing two parameterised models based on the seizure's spectral patterns (Fig. 1): beta and gamma bands power, and cross-spectral principal component analysis (PCA).

The EEG quantification window was defined as the period from 30 s prior to the ictal onset to the time of seizure termination. Four electrode contacts of interest were identified for this analysis: RA electrode contact 1 (RA1), RH electrode contact 1 (RH1), LA electrode contact 1 (LA1) and LAH electrode contact 2 (LAH2). A Morlet wavelet transform (Tallon-Baudry et al., 1998) was used to calculate the spectral power density in 1 Hz intervals in the range: 1–120 Hz. The resulting time courses were converted into a z-score for each frequency and convolved with the canonical HRF (see Fig. 1).

- *Model 3 Beta and gamma bands power model*: this model is designed to reflect the visual prominence of beta and gamma activities during the seizure. Two sets of 4 regressors, 4 for the beta band (15–35 Hz) and 4 for the gamma band (40–120 Hz), were defined based on the EEG at each of the four electrode contacts of interest; for each 1 Hz interval the power as a function of time at each channel was convolved with the canonical HRF, and averaged across intervals for each band.
- *Model 4 Cross-spectral PCA model*: this model is designed to quantify the prominent spectral dynamics, and allows the characterisation of power and frequency shifts. A PCA of the power spectrogram was performed and the components that account for 90% of the variance were identified and used as regressors of interest to model BOLD changes. Model 4 was defined for each of the four electrode contacts of interest. Depending on the EEG channel between 4 and 6 components were found to describe 90% of the variance.

For all models, inter-scan realignment parameters and their Volterra expansion (Friston et al., 1996), cardiac pulse (Liston et al., 2006) and IED were included in the design matrices for seizure spectral dynamics as confounds.

2.6. Assessment of the BOLD changes

SPMs were obtained for the ictal and preictal phases (models 1 and 2), beta and gamma powers (model 3) across the principal component regressors (model 4) for each electrode of interest using appropriate F contrasts. For each effect of interest, the presence of significant BOLD changes was assessed over the whole brain at a statistical threshold of $p < 0.001$ (uncorrected for multiple comparisons) and a cluster size threshold of 5 contiguous voxels (Chaudhary et al., 2012; Zijlmans et al., 2007; Pittau et al., 2012; Donaire et al., 2009). The resulting maps were co-registered with the T1-weighted MRI scan using rigid-body co-registration in SPM, and were classified as either *Entirely Concordant*, *Concordant Plus*, *Some Concordance* and *Discordant* based on the location of global statistical maximum (GM) BOLD cluster and other BOLD clusters in relation to the SOZ for seizure (Chaudhary et al., 2012).

3. Results

3.1. BOLD changes for visual segmentation of ictal phases and IEDs (models 1 and 2)

No significant changes were observed for the *preictal phase* (Fig. 2; Table 2). Significant BOLD changes for the *ictal onset phase* were seen in right temporal lobe (TL) involving both medial (temporal pole/fusiform gyrus) and lateral structures, and regions belonging to

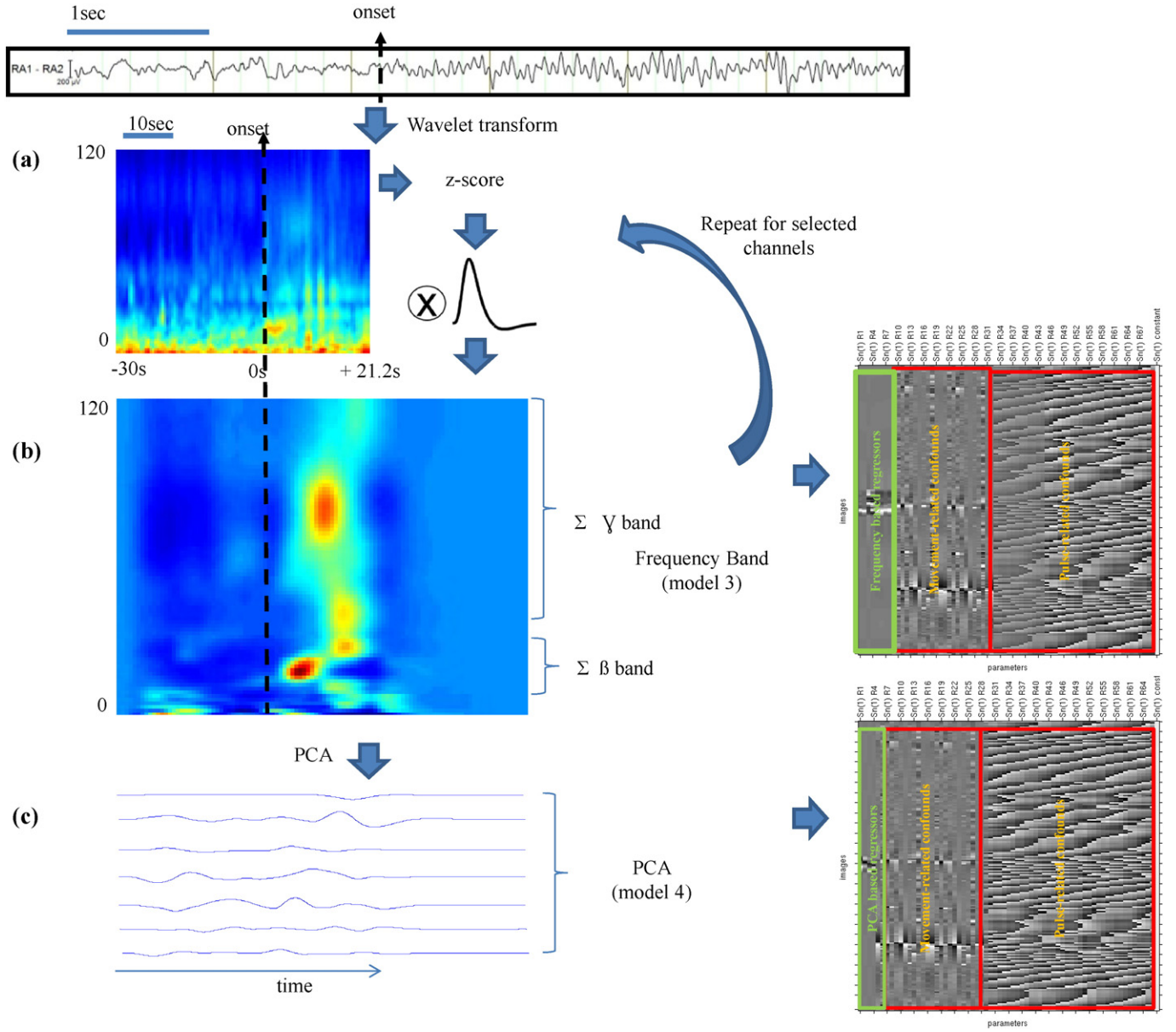

Fig. 1. fMRI model derivation from EEG frequency decomposition (models 3 and 4). (a) Data from a selected contact (e.g. in the figure right amygdala showing sz onset) for the pre-ictal (−30 s from seizure onset) and ictal phase (+21.2 s from seizure onset) was wavelet transformed to a representation in time (x) and frequency (y). (b) The data was convolved with a haemodynamic response and averaged within the beta and gamma bands. This procedure was repeated for each channel and the resulting regressors were entered into a design matrix (model 3). (c) A principal component analysis was performed to reduce the time-frequency data into the smallest number of regressors able to explain 90% of the data variance. These regressors were the effects of interest in model 4.

the default mode network (DMN). For the *late ictal phase* significant changes were located in the right hemisphere remote from SOZ (*right* occipital and DMN regions). The maps were classified as *Concordant Plus* and *Discordant* respectively.

3.2. BOLD changes for seizure spectral dynamics (models 3 and 4)

For model 3, beta power across all four electrodes was associated with significant BOLD increases in the frontal lobe regions (L inferior frontal gyrus and R frontal pole), classified as *Discordant* (Fig. 3aii). Gamma power was associated with significant BOLD changes in the R hippocampus and frontal lobe areas (R frontal pole, L inferior and L superior frontal gyrus) (Table 3, Fig. 3ai), and classified as *Concordant Plus*.

For model 4, significant BOLD changes were revealed in the R hippocampus/amygdala and fusiform gyrus, and in the left and right frontal lobes, for 3 out of the 4 electrodes of interest: RH1, LA1, LAH2 (Fig. 3b; Table 3). No significant activations were revealed for model 4 for RA1. The LA1 map was classified as *Concordant Plus* and the RH1 and LAH2 maps were classified as *Some Concordance*.

(For the BOLD maps associated with individual PCs see Supplementary Table S1, Figs. S1–S4).

4. Discussion

To our knowledge this is the first report of BOLD changes associated with an electrographic seizure recorded from the right temporal lobe on icEEG. This presents us with an opportunity to investigate the brain networks involved in the transition from interictal to ictal state and propagation over the entire brain and to investigate the correlates of BLOD changes to the different EEG modelling approaches.

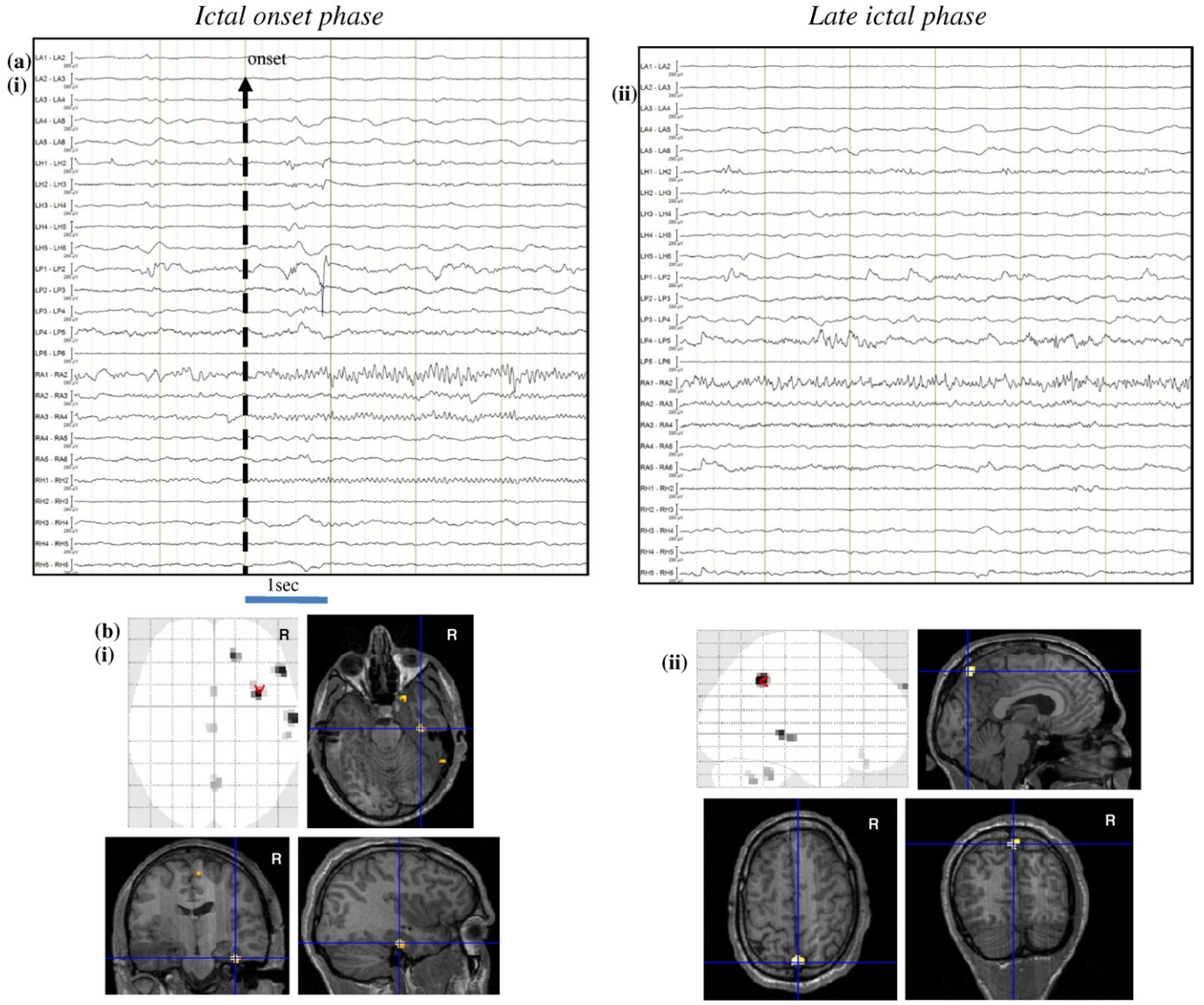

Fig. 2. Seizure-related BOLD changes based on visual segmentation of seizure (models 1 and 2). (a) Representative sample of EEG recorded during icEEG-fMRI, (i) EEG showing *Ictal onset phase* consisted of fast activity in beta range involving RA contacts 1–4 and RH contacts 1–2. (ii) EEG showing Late-ictal phase consisted of fast activity in gamma range involving RA contacts 1–2 and LPH contacts 4–5. (b) BOLD changes overlaid on glass brain and on a co-registered T1-volume. (i) *Ictal onset phase*-related BOLD clusters were seen in the right fusiform gyrus (global statistical maximum: cross-hair) in addition to other clusters in the right temporal lobe and the precuneus. (ii) Late-ictal phase-related BOLD clusters were seen in the precuneus (global statistical maximum: cross-hair) in addition to other clusters in the right temporal lobe and the posterior cingulate.

The main findings derived from the different models are:

- Visually identified phases (model 1) showed significant BOLD signal changes in the right temporal lobe for the *ictal onset phase* and a widespread network for the *late ictal phase.*
- Quantitative analysis of EEG (models 3 and 4) across the period covering the pre-ictal and ictal phase was more sensitive to activity in the key structures of SOZ (amygdala and hippocampus) than the visual approach. In particular BOLD changes related to the PCs, and to a lesser extent to gamma band power, showed significant activity in SOZ next to the active electrodes.
- Additional regions beyond the seizure onset zone and not covered by the intracranial recording were consistently revealed across the different analyses. These include right fusiform gyrus, and frontal lateral and orbitofrontal cortices, and areas belonging to the DMN, suggesting these areas may be part of the epileptogenic network.

4.1. Methodological aspects

We followed a strict icEEG-fMRI safety protocol (Carmichael et al., 2008, 2010) and EEG data quality was sufficient for meaningful quantification. Some MRI signal dropout was observed within 1 cm around implanted electrodes in the amygdalae and hippocampi, which can significantly limit BOLD sensitivity in these regions (Carmichael et al., 2012). Intracranial EEG has high sensitivity allowing identification of very focal epileptic events including seizures and interictal discharges, and therefore may be associated with relatively weak BOLD changes. Nonetheless, we found significant BOLD changes in the SOZ, in line with previous findings (Vulliemoz et al., 2011; Cunningham et al., 2012).

Our two-pronged fMRI mapping strategy was designed to use human expert knowledge (visual ictal phases identification plus preictal period: models 1 and 2 (Chaudhary et al., 2012)) on one hand and, given the recognised importance of certain EEG rhythms during seizures and

Table 2
Seizure-related BOLD changes using visual based modelling of EEG (model 1).

Ictal phases	BOLD changes							Seizure onset zone	Level of concordance
	Left hemisphere			Right hemisphere			Deep structures		
	Temporal	Frontal	Parietal	Temporal	Frontal	Parietal			
Ictal-onset phase (model 1)				R temporal pole, **fusiform gyrus**[a], MTG[a]			Posterior cingulate	Right amygdala/hippocampus	C+
Late-ictal phase (model 1)				Posterior temporal			**Precuneus,** posterior cingulate		D

Abbreviations: MTG = middle temporal gyrus, MFG = middle frontal gyrus, LAH = left anterior hippocampus, C+ = concordant plus, and D = discordant.
Global maximum statistical cluster shown in **bold**.
[a] FEW $p < 0.05$ corrected.

the very direct measurement provided by icEEG, to assess the value of a more quantitative BOLD predictors on the other, and to compare the two approaches. Beta and gamma band activities are often associated with ictal events at seizure onset (Bartolomei et al., 2004; David et al., 2011) and were visually evident during the seizure under investigation. We therefore used signal power in these two EEG frequency bands to derive BOLD predictors that can be modulated within and across ictal phases (model 3) (in contrast to variable-duration fixed-amplitude blocks for models 1 and 2) over the entire duration of the combined preictal and ictal phases.

In a further more data-driven modelling approach (model 4), we wanted to explore a model incorporating activity over the full range of frequencies to attempt to capture the most prominent shifts in frequency during the event. To this effect, we performed PCA of the spectrogram, taking care of normalising to account for the EEG's 1/f power distribution. Our quantitative approach focused on the four EEG electrode contacts located in the mesial temporal structures bilaterally: RA and RH within the SOZ and LA and LAH contralaterally, because of their clear epileptogenic role, confirmed by surgical outcome and given the gradual spread of the ictal activity in those channels.

4.2. Biological significance

We found that *ictal onset phase*-related BOLD maps were more closely co-localised with the SOZ and all the clusters of activity but one were located in the right temporal lobe compared to *late ictal phase* related maps which showed widespread activity. This is in line with our own (Chaudhary et al., 2012; Thornton et al., 2010) and other (Donaire et al., 2009; Tyvaert et al., 2009) findings using scalp EEG-fMRI in patients with refractory focal epilepsy. The regions revealed in the early ictal phase go in accordance with the findings that organized networks in medial and lateral temporal lobe are at play in the process of seizure generation in medial temporal lobe seizures (Bartolomei et al., 2001).

However, BOLD signal changes in the key structures involved in seizure generation (amygdala and hippocampus) were only captured by the quantitative models (models 3 and 4). In particular, the PCs of the EEG signal across the period covering the pre-ictal and ictal phases revealed the strongest activity clusters in the regions of electrode placement followed by gamma power fluctuations.

Several factors can offer an explanation to these findings and the differences observed between models. For the visual analysis, the seizure is

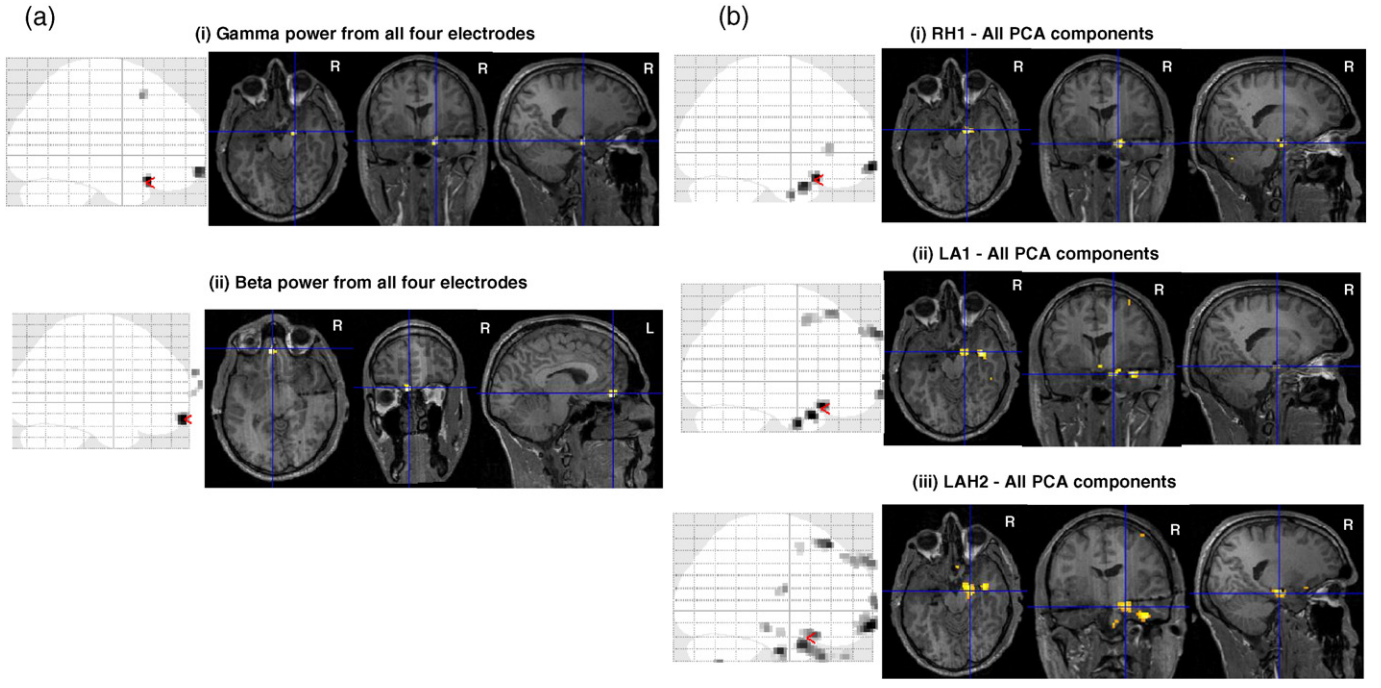

Fig. 3. Seizure-related BOLD changes based on seizure spectral dynamics (models 3 and 4). BOLD changes overlaid on glass brain (sagittal slice) and on a co-registered T1-volume. (a)(i) gamma power from all four electrode contacts showed changes in right hippocampus (red marker on sagittal slice of glass brain and cross hair on T1-volume); (ii) beta power from all four electrode contacts showed changes in left orbitofrontal cortex (red marker on sagittal slice of glass brain, cross hair on T1-volume). (b) BOLD changes for model 4: (i) all PCA components from electrode contact RH1 in right hippocampus and left orbitofrontal cortex (ii) all PCA components from electrode contact LA1 in the right fusiform gyrus and right hippocampus (iii) all PCA components from electrode contact LAH2 in the right hippocampus and right fusiform gyrus and left orbitofrontal cortex (red marks in crystal brain and crosshair correspondence).

Table 3
Seizure-related BOLD changes using time-frequency based modelling of EEG (models 3 and 4).

Model	Electrode contact	Contrast type	BOLD changes								Level of concordance
			Right				Left				
			Frontal	Parietal	Temporal	Occipital	Frontal	Parietal	Temporal	Occipital	
Model 3	RA1 + RH1 + LA1 + LAH2	Gamma	Medial SFG		**Amygdala/hippocampus**		OF/SFG				C+
		Beta	Medial SFG MFG				**OF**				D
Model 4	RA1	All PCAs	–	–	–	–	–	–	–	–	–
	RH1	All PCAs			Amygdala/hippocampus, fusiform		**OF**[a], IFG				SC
	LA1	All PCAs	OF,MFG		Amygdala/hippocampus, **fusiform**[a]		OF				C+
	LAH2	All PCAs	OF,MFG*		Amygdala/hippocampus, fusiform[a]		**OF**[a], **MFG**				SC

Abbreviations: MTG = middle temporal gyrus, MFG = middle frontal gyrus, IFG = inferior frontal gyrus, SFG = superior frontal gyrus, OF = orbitofrontal, LAH = left anterior hippocampus, LA = left amygdala, RA = right amygdala, and RH = right hippocampus.
C+ = concordant plus, SC = some concordance, and D = discordant.
Global maximum statistical cluster shown in **bold**.
[a] Clusters survive FEW $p < 0.05$.

segmented in different phases according to the prominent rhythms, which is subjective, and one phase is explored at a time. While this approach creates a potentially more clinically-relevant hypothesis about seizure dynamics this segmentation process, by forcing a categorisation, may ignore crucial information contained on the EEG that relates to the activity in the key structures of SOZ. In this case study, *ictal onset* and *late ictal phases* revealed the specific regions that are differently involved for each phase: a set of regions in the medial and lateral right TL is involved in the onset and a widespread network is related to the late phase. However the activity in amygdala and hippocampus was only revealed when the entire pre-ictal and ictal period was examined and the EEG information was summarized in PCs or band fluctuations.

As noted, the two quantitative models, capture signal variations across the whole pre-ictal and ictal period (51.2 s). The highest sensitivity to BOLD changes in the hippocampal/amygdala region was achieved by the PCs of the spectral decomposition of the seizure (model 4). The PCs encapsulate the main features across the EEG spectrogram, suggesting that the BOLD signal changes in the SOZ structures are better explained by a combination of EEG features across bands and phases than the individual ictal phases. We note that the results were similar between the different electrode contacts, most likely because they all record the main seizure features.

From the two EEG bands analysed, gamma power fluctuations showed a significant correlation with the SOZ structures while beta activity related to frontal regions. Gamma activity has been reported to be the band that better explains BOLD signal changes in a large range of brain networks (Laufs, 2008), this could offer an explanation of why gamma fluctuations extracted from the electrodes in amygdala and hippocampus during the preictal and ictal period may correlate better with BOLD signal in this structures compared with beta. It is also of note that following convention, the gamma band model covers a wider part of the spectrum (40–120 Hz) than the beta (1–35 Hz) and therefore may encapsulate a greater amount of EEG information.

In addition to BOLD changes in the SOZ, significant changes were seen in the remote cortical areas including the right fusiform gyrus, orbito frontal cortex and areas belonging to the default mode network for visual based and spectral dynamics based modelling. These findings are in agreement with previous scalp EEG-fMRI studies (Laufs et al., 2007) and raise the question regarding role of these structures in the seizure generation and propagation. The precuneus has been shown to play an important role in the generation/maintenance of generalized spike wave discharges (Vaudano et al., 2009). We suggest that it may also have important role to play in focal seizure generation and spread in line with previous findings in focal refractory seizures using scalp EEG-fMRI (Chaudhary et al., 2012; Donaire et al., 2009; Tyvaert et al., 2009). Regions such as the orbitofrontal cortex and cingulate have been suggested to participate in the inter-hemispheric spread of medial temporal lobe seizures (Chabardes et al., 2005; Lieb et al., 1991; Lieb and Babb, 1986; Laufs et al., 2011).

4.3. Quantitative vs qualitative models

We suggest that beta and gamma band power and PCs of the spectral decomposition of the seizure represent a relatively unbiased modelling approach to characterise ictal dynamics locally and remotely with higher sensitivity than based on a more conventional, visual based segmentation of the ictal event. This is at the slight cost of losing a direct link with the expert visual description of the seizure evolution which by taking into account the spatiotemporal and electroclinical characteristics, can attempt to separate the ictal onset related BOLD changes from propagation related BOLD changes. We also suggest that the availability of icEEG data makes a quantitative approach more suitable for concurrent fMRI modelling compared to scalp EEG.

5. Conclusions

In conclusion icEEG-fMRI allowed us to reveal BOLD changes within and beyond the SOZ linked to very localised ictal fluctuations in beta and gamma activity measured in the amygdala and hippocampus. Furthermore, the BOLD changes within the SOZ structures were better captured by the quantitative models, highlighting the interest in considering seizure-related EEG fluctuations across the entire spectrum.

Supplementary data to this article can be found online at http://dx.doi.org/10.1016/j.nicl.2016.03.010.

Acknowledgement

This work was partly funded through grants and bursaries from the Medical Research Council (MRC grant number G0301067), Action Medical Research (SP4646), Swiss National Science Foundation (SNF grant 141165) and the support of UCL Institute of Neurology. This work was undertaken at UCLH/UCL who received a proportion of funding from the Department of Health's NIHR Biomedical Research Centres funding scheme. We are grateful to the radiographers: Lisa Strycharczuk, Bruce Metheringham and Alison Duncan, and the MR physicists Mark White and Laura Manchini of the Lysholm Department of Neuroradiology and Neurophysics at the National Hospital for Neurology and Neurosurgery (UCLH NHS Foundation Trust), for their expert scanning assistance.

References

Allen, P.J., Josephs, O., Turner, R., 2000. A method for removing imaging artifact from continuous EEG recorded during functional MRI. NeuroImage 12, 230–239.

Babb, T.L., Wilson, C.L., Isokawa-Akesson, M., 1987. Firing patterns of human limbic neurons during stereoencephalography (SEEG) and clinical temporal lobe seizures. Electroencephalogr. Clin. Neurophysiol. 66, 467–482.
Bartolomei, F., Wendling, F., Bellanger, J.J., Regis, J., Chauvel, P., 2001. Neural networks involving the medial temporal structures in temporal lobe epilepsy. Clin. Neurophysiol. 112, 1746–1760.
Bartolomei, F., Wendling, F., Regis, J., Gavaret, M., Guye, M., Chauvel, P., 2004. Pre-ictal synchronicity in limbic networks of mesial temporal lobe epilepsy. Epilepsy Res. 61, 89–104.
Carmichael, D.W., Thornton, J.S., Rodionov, R., et al., 2008. Safety of localizing epilepsy monitoring intracranial electroencephalograph electrodes using MRI: radiofrequency-induced heating. J. Magn. Reson. Imaging 28, 1233–1244.
Carmichael, D.W., Thornton, J.S., Rodionov, R., et al., 2010. Feasibility of simultaneous intracranial EEG-fMRI in humans: a safety study. NeuroImage 49, 379–390.
Carmichael, D.W., Vulliemoz, S., Rodionov, R., Thornton, J.S., McEvoy, A.W., Lemieux, L., 2012. Simultaneous intracranial EEG-fMRI in humans: data quality. NeuroImage.
Chabardes, S., Kahane, P., Minotti, L., et al., 2005. The temporopolar cortex plays a pivotal role in temporal lobe seizures. Brain 128, 1818–1831.
Chaudhary, U.J., Carmichael, D.W., Rodionov, R., et al., 2012. Mapping preictal and ictal haemodynamic networks using video-electroencephalography and functional imaging. Brain 135, 3645–3663.
Cunningham, C.B., Goodyear, B.G., Badawy, R., et al., 2012. Intracranial EEG-fMRI analysis of focal epileptiform discharges in humans. Epilepsia 53, 1636–1648.
deCurtis, M., Gnatkovsky, V., 2009. Reevaluating the mechanisms of focal ictogenesis: the role of low-voltage fast activity. Epilepsia 50, 2514–2525.
David, O., Blauwblomme, T., Job, A.S., et al., 2011. Imaging the seizure onset zone with stereo-electroencephalography. Brain 134, 2898–2911.
Donaire, A., Bargallo, N., Falcon, C., et al., 2009. Identifying the structures involved in seizure generation using sequential analysis of ictal-fMRI data. NeuroImage 47, 173–183.
Fisher, R.S., van Emde, Boas W., Blume, W., et al., 2005. Epileptic seizures and epilepsy: definitions proposed by the International League Against Epilepsy (ILAE) and the International Bureau for Epilepsy (IBE). Epilepsia 46, 470–472.
Friston, K.J., Holmes, A.P., Worsley, K.J., Poline, J.B., Firth, C.D., Frackowiak, R.S.J., 1995. Statistical parametric maps in functional imaging: a general linear approach. Hum. Brain Mapp. 2, 189–210.
Friston, K.J., Jezzard, P., Turner, R., 1994. Analysis of functional MRI time series. Hum. Brain Mapp. 1, 153–171.
Friston, K.J., Williams, S., Howard, R., Frackowiak, R.S., Turner, R., 1996. Movement-related effects in fMRI time-series. Magn. Reson. Med. 35, 346–355.
Gnatkovsky, V., Librizzi, L., Trombin, F., de C, M., 2008. Fast activity at seizure onset is mediated by inhibitory circuits in the entorhinal cortex in vitro. Ann. Neurol. 64, 674–686.
Laufs, H., Hamandi, K., Salek-Haddadi, A., Kleinschmidt, A.K., Duncan, J.S., Lemieux, L., 2007. Temporal lobe interictal epileptic discharges affect cerebral activity in "default mode" brain regions. Hum. Brain Mapp. 28, 1023–1032.
Laufs, H., Richardson, M.P., Salek-Haddadi, A., et al., 2011. Converging PET and fMRI evidence for a common area involved in human focal epilepsies. Neurology 77, 904–910.
Laufs, H., 2008. Endogenous brain oscillations and related networks detected by surface EEG-combined fMRI. Hum. Brain Mapp. 29, 762–769.
Lieb, J.P., Babb, T.L., 1986. Interhemispheric propagation time of human hippocampal seizures: II. Relationship to pathology and cell density. Epilepsia 27, 294–300.
Lieb, J.P., Dasheiff, R.M., Engel Jr., J., 1991. Role of the frontal lobes in the propagation of mesial temporal lobe seizures. Epilepsia 32, 822–837.
Liston, A.D., Lund, T.E., Salek-Haddadi, A., Hamandi, K., Friston, K.J., Lemieux, L., 2006. Modelling cardiac signal as a confound in EEG-fMRI and its application in focal epilepsy studies. NeuroImage 30, 827–834.
Mormann, F., Kreuz, T., Andrzejak, R.G., David, P., Lehnertz, K., Elger, C.E., 2003. Epileptic seizures are preceded by a decrease in synchronization. Epilepsy Res. 53, 173–185.
Niedermeyer, E., Lopes da Silva, F.H., 2005. Electroencephalography: Basic Principles, Clinical Applications, and Related Fields. 5th ed. Lippincott Williams & Wilkins, Philadelphia.
Pittau, F., Dubeau, F., Gotman, J., 2012. Contribution of EEG/fMRI to the definition of the epileptic focus. Neurology 78, 1479–1487.
Schindler, K., Leung, H., Elger, C.E., Lehnertz, K., 2007. Assessing seizure dynamics by analysing the correlation structure of multichannel intracranial EEG. Brain 130, 65–77.
Smith, S.J., 2005. EEG in the diagnosis, classification, and management of patients with epilepsy. J. Neurol. Neurosurg. Psychiatry 76 (Suppl. 2), ii2–ii7.
Tallon-Baudry, C., Bertrand, O., Peronnet, F., Pernier, J., 1998. Induced gamma-band activity during the delay of a visual short-term memory task in humans. J. Neurosci. 18, 4244–4254.
Tao, J.X., Baldwin, M., Ray, A., Hawes-Ebersole, S., Ebersole, J.S., 2007. The impact of cerebral source area and synchrony on recording scalp electroencephalography ictal patterns. Epilepsia 48, 2167–2176.
Thornton, R., Vulliemoz, S., Rodionov, R., et al., 2011. Epileptic networks in focal cortical dysplasia revealed using electroencephalography-functional magnetic resonance imaging. Ann. Neurol. 70, 822–837.
Thornton, R.C., Rodionov, R., Laufs, H., et al., 2010. Imaging haemodynamic changes related to seizures: comparison of EEG-based general linear model, independent component analysis of fMRI and intracranial EEG. NeuroImage 53, 196–205.
Truccolo, W., Donoghue, J.A., Hochberg, L.R., et al., 2011. Single-neuron dynamics in human focal epilepsy. Nat. Neurosci. 14, 635–641.
Tyvaert, L., Hawco, C., Kobayashi, E., LeVan, P., Dubeau, F., Gotman, J., 2008. Different structures involved during ictal and interictal epileptic activity in malformations of cortical development: an EEG-fMRI study. Brain 131, 2042–2060.
Tyvaert, L., LeVan, P., Dubeau, F., Gotman, J., 2009. Noninvasive dynamic imaging of seizures in epileptic patients. Hum. Brain Mapp. 30, 3993–4011.
Vaudano, A.E., Laufs, H., Kiebel, S.J., et al., 2009. Causal hierarchy within the thalamo-cortical network in spike and wave discharges. PLoS One 4, e6475.
Vulliemoz, S., Carmichael, D.W., Rosenkranz, K., et al., 2011. Simultaneous intracranial EEG and fMRI of interictal epileptic discharges in humans. NeuroImage 54, 182–190.
Wendling, F., Bartolomei, F., Bellanger, J.J., Bourien, J., Chauvel, P., 2003. Epileptic fast intracerebral EEG activity: evidence for spatial decorrelation at seizure onset. Brain 126, 1449–1459.
Zijlmans, M., Huiskamp, G., Hersevoort, M., Seppenwoolde, J.H., van Huffelen, A.C., Leijten, F.S., 2007. EEG-fMRI in the preoperative work-up for epilepsy surgery. Brain 130, 2343–2353.